Results of Pioneer-Venus 1978 Sequential Decoding Tests Over a Simulated Lognormal Fading Channel

B. K. Levitt
Communications Systems Research Section

Tests were performed in 1976 at the Jet Propulsion Laboratory's Compatibility Test Area (CTA 21) to investigate the effects of lognormal fading on Pioneer-Venus 1978 (PV78) sequential decoding performance. The results of these simulations were used to refine a previously developed empirical model for predicting PV78 telemetry link performance.

I. Introduction

The PV78 orbiter will dispatch several probes into the planet atmosphere. The telemetry from these probes will be transmitted directly to Earth at data rates between 16 and 256 b/s over a coherent, binary PSK link using a (32, 1/2) convolutional code. These communication links will be degraded by lognormal fading due to turbulence in the atmosphere of Venus (Refs. 1, 2).

In connection with the Helios mission, Layland developed a medium-rate empirical model for analytically determining the effects of a noisy carrier reference on coherent, sequential decoding performance (Ref. 3). For PV78 applications, this model was modified to include the additional degradation of lognormal fading (Ref. 4). However, the accuracy of this extended fading/noisy reference model had not been verified experimentally. Moreover, although many individual decisions over widely varying time intervals are made in sequentially decoding a frame of received data, the models characterized these decoder integration times by a *single* effective interval T_m. In his pioneering work, Layland used a value of T_m which was approximately twice the bit time T_b (Ref. 3, Eq. 4). Still, it was believed that T_m/T_b was a function of the data rate (Ref. 5, Sect. III), and that a more accurate empirical model could be produced by selecting the value of this parameter that provided the closest agreement with experimental deletion rate behavior (Ref. 4, Sect. IV).

With these considerations, tests were conducted in CTA 21 for several months during 1976 to gather experimental data on the performance of PV78 sequentially decoded telemetry at 256 b/s, with and without simulated lognormal fading. This report describes the results of that effort.

II. Test Procedure

Tests were performed using the standard DSN transmitter/receiver configuration in CTA 21, modified to accommodate the simulated channel fading. Specifically, as shown in Figure 1, the test equipment included the Simulation Conversion Assembly (SCA), a test transmitter, a PIN attenuator modulated by a Gaussian noise generator to simulate lognormal fading (see Appendix), the Y-Factor Assembly (YFA), a DSN Block III receiver, the Subcarrier Demodulator Assembly (SDA), two Symbol Synchronizer Assemblies (SSA's), two

Telemetry/Command Processors (TCP's), the Data Decoder Assembly (DDA), and a magnetic tape unit which provided the test output Original Data Record (ODR).

The SCA supplied a pseudorandom data sequence to the test transmitter. The (32, 1/2) convolutionally coded data was biphase – modulated onto a 32.768 KHz squarewave subcarrier, which in turn phase-modulated the S-band carrier at the test transmitter. The carrier modulation index θ was set at the test transmitter before each test. The data rate for all tests was 256 b/s.

Based on previous experience, the PIN attenuator had a tendency to drift until it reached its ambient operating temperature: consequently, it was always turned on at least 24 hours prior to a test. With the noise generator off, and the attenuator at its d.c. bias point, the "received" signal-to-noise ratio was set to its approximate test level using the Y-factor measurement technique (Ref. 6). If the test specified log-normal fading with logamplitude variance σ_χ^2, the Gaussian noise generator was then set to a corresponding signal level which depended on the PIN attenuator input/output characteristic slope (see Appendix). A 1 Hz lowpass filter was inserted at the output of the noise generator to simulate the fading bandwidth of the Venus atmosphere (Ref. 1, p. 38, and Ref. 2, p. 45). The received symbol error rate (SER) was then observed on the SSA-TCP monitoring string, and fine adjustments were made in the received signal strength until the predetermined test SER was achieved. The tape unit was then engaged, and test data was collected, usually for several hours to ensure statistical validity.

The SSA-DDA-TCP string operated in real time to provide the ODR with a listing of the number of computations required to sequentially decode each frame of received data, or an indication that a particular frame had been deleted because the system capacity of 25000 computations per second (or about 100 computations per bit at 256 b/s) had been exceeded. Later, off-line computer processing of the ODR determined the test frame deletion rate characteristic as a function of computational speed, up to the real-time sequential decoder limit. The other SSA-TCP string was used to monitor the telemetry channel by identifying drifts in SER and received symbol signal-to-noise ratio due to fluctuations in station parameters.

III. Test Results

The results of these tests are summarized in Table 1. Of the 16 satisfactorily completed runs, 6 involved simulated log-normal fading with $\sigma_\chi^2 = .049$, which is the level of fading anticipated in the limiting case of a PV78 probe transmitting from the surface of Venus to Earth in a direction 60° off vertical (Ref. 5, p. 53). Two runs were made at each modulation index θ; in both the fading and non-fading cases, the central values of θ were selected because they were near optimum in the sense that the PV78 link design deletion rate of 10^{-2} could be achieved with minimum signal power. The received signal-to-noise level, as evidenced by the measured SER, was selected for each test to produce a frame deletion rate in the vicinity of 10^{-2}, based on empirical predictions. Ten independent measurements of SER were made before and after each run, and the average of these is recorded as AVG SER in Table 1.

Prior to the sequential decoding efforts, models had been developed for determining the bit error rate of uncoded, coherent binary PSK telemetry with a noisy carrier reference, with and without fading (Refs. 2, 7). These uncoded models do not have the problem of a variable integration time, characterized by T_m in the sequential decoding case. Consequently, these models are inherently more accurate than their successors, particularly at medium data rates where the bit detection time T_b is on the order of the coherence time of the noisy carrier reference and the channel fading. Based on these uncoded models, curves of SER versus θ were plotted in Figs. 2 and 3 for various signal-to-noise ratios (defined as received signal power P/noise spectral power density N_0). These plots were used to convert the AVG SER's into experimental (EXP) SNR's in Table 1. It is believed that these SNR's are more representative of the actual test values than those derived by the Y-factor method. A basic premise inherent in Figs. 2 and 3, and the work that follows, is that the carrier and data channel losses (I_C and L_D) in the test equipment due to predetection recording, waveform distortion, SSA, and SDA are given by the PV78 design values of 1.00 and 2.08 dB respectively (Ref. 5, p. 52).

Off-line processing of the ODR's generated the plots of experimental frame deletion rate versus sequential decoder computational rate N, in computations/bit, indicated by the X's in Fig. 4. A smooth curve (not shown in Fig. 4) was drawn through the experimental data for each run, and values of the deletion rate at $N = 5$ and $N = 100$ computations/bit were read off these curves and recorded in Table 1. The sequential decoding performance models of Refs. 3 and 4 compute T_m according to the formula (Ref. 4, Eq. 5)

$$T_m = KT_b \left[1 - \frac{1}{N}\log_2 \left(1 + \frac{N}{2}\right)\right] \quad ; K = 2 \qquad (1)$$

One of the objectives of these tests was to determine whether some other value of K ($\cong T_m/T_b$ for large N) would provide better agreement between the empirical models and experimental data. To this end, the distance parameter

$$D(K) = \sum_{\text{run}=1}^{16} \sum_{N=5,100} \left[\log_{10} \frac{\text{EMP. DELETION RATE}(K)}{\text{EXP. DELETION RATE}} \right]^2 \quad (2)$$

was computed over a range of K, where the numerator of the argument above was based on a generalized version of the models in Refs. 3 and 4, with arbitrary K, with P/N_0 given by the EXP SNR values in Table 1, and with telemetry carrier and data channel losses L_C = 1.00 dB and L_D = 2.08 dB. As shown in Fig. 5, $D(K)$ was minimized near K = 7.

The modified sequential decoding models with K = 7 were used to generate the deletion rate versus modulation index and received SNR curves of Figs. 6 and 7, for the PV78 computational rate N = 100 computations/bit. The experimental deletion rates in Table 1 at this value of N were superimposed on these curves, yielding the empirical (EMP) SNR's recorded in Table 1.

The difference ΔSNR $\equiv$ EMP SNR − EXP SNR is a measure of the accuracy of these modified performance models. Based on the 16 test runs, ΔSNR has a mean of −.11 dB and a standard deviation of .33 dB. The negative mean indicates that the sequential decoding models are optimistic, tending to underestimate the SNR required to achieve a given deletion rate. The models have an apparent accuracy of about .4 − .5 dB (|mean| + standard deviation), and part of this error may be due to incorrect estimates of the telemetry channel losses.

Acknowledgement

This technique for simulating lognormal channel fading was developed by W. J. Hurd, and hardware implementation was provided by W. P. Hubbard, both of Section 331 at Jet Propulsion Laboratory.

References

1. Woo, R., et al., *Effects of Turbulence in the Atmosphere of Venus on Pioneer Venus Radio – Phase 1,* Technical Memorandum 33-644, Jet Propulsion Laboratory, Pasadena, Calif., June 30, 1973.

2. Levitt, B. K., and Rhee, M. Y., "Effects of Lognormal Amplitude Fading on Bit Error Probability for Uncoded Binary PSK Signalling," in *The Deep Space Network Progress Report 42-21,* pp. 45-54, Jet Propulsion Laboratory, Pasadena, Calif., June 15, 1974.

3. Layland, J. W., "A Sequential Decoding Medium-Rate Performance Model," in *The Deep Space Network, Technical Report 32-1526,* Vol. XVIII, pp. 29-40, Jet Propulsion Laboratory, Pasadena, Calif., December 15, 1973.

4. Levitt, B. K., "Performance Degradation of Uncoded and Sequentially Decoded PSK Systems Due to Lognormal Fading," in *The Deep Space Network Progress Report 42-32,* pp. 58-67, Jet Propulsion Laboratory, Pasadena, Calif., October 15, 1974.

5. Levitt, B. K., "Pioneer Venus 1978: Telemetry Performance Predicts," in *The Deep Space Network Progress Report 42-24,* pp. 51-59, Jet Propulsion Laboratory, Pasadena, Calif., December 15, 1974.

6. DSIF Program Library, Documentation for Y-Factor Computer Program, DOI-5343-SP-B, Jet Propulsion Laboratory, Pasadena, Calif., September 29, 1972 (JPL internal document).

7. Layland, J. W., "A Note on Noisy Reference Detection," in *The Deep Space Network,* Technical Report 32-1526, Vol. XVII, pp. 83-88, Jet Propulsion Laboratory, Pasadena, Calif., October 15, 1973.

Table 1. Sequential Decoding Test Results

σ_x^2	θ°	Run	Avg. SER $\times 10^{-2}$	Exp. SNR dB	Experimental Frame Deletion Rate @ N = 5 Comp/Bit	Experimental Frame Deletion Rate @ N = 100 Comp/Bit	Emp. SNR dB	ΔSNR dB
0	48	1	9.22	31.51	2.89×10^{-1}	1.25×10^{-2}	31.72	.21
		2	9.73	31.32	6.2×10^{-1}	5.9×10^{-2}	31.30	−.02
	53	3	7.29	31.72	1.08×10^{-1}	3.7×10^{-3}	31.59	−.13
		4	7.61	31.58	4.2×10^{-2}	8.0×10^{-4}	31.96	.38
	58	5	6.73	31.52	7.5×10^{-2}	3.5×10^{-3}	31.43	−.09
		6	6.48	31.63	3.9×10^{-2}	1.6×10^{-3}	31.66	.03
	63	7	5.88	31.57	5.7×10^{-2}	3.3×10^{-3}	31.54	−.03
		8	5.81	31.60	1.85×10^{-2}	1.0×10^{-3}	31.96	.36
	68	9	5.40	31.62	1.55×10^{-1}	1.6×10^{-2}	31.17	−.45
		10	5.49	31.58	9.0×10^{-2}	6.7×10^{-3}	31.61	.03
.049	59	11	2.70	34.53	6.3×10^{-2}	7.2×10^{-3}	34.66	.13
		12	2.50	34.70	8.8×10^{-2}	1.5×10^{-2}	34.16	−.54
	64	13	2.33	34.54	8.9×10^{-2}	1.8×10^{-2}	33.80	−.74
		14	2.02	34.83	5.9×10^{-2}	5.1×10^{-3}	34.74	−.09
	69	15	2.27	34.44	8.8×10^{-2}	1.3×10^{-2}	34.06	−.38
		16	2.63	34.13	6.0×10^{-2}	2.0×10^{-2}	33.71	−.42

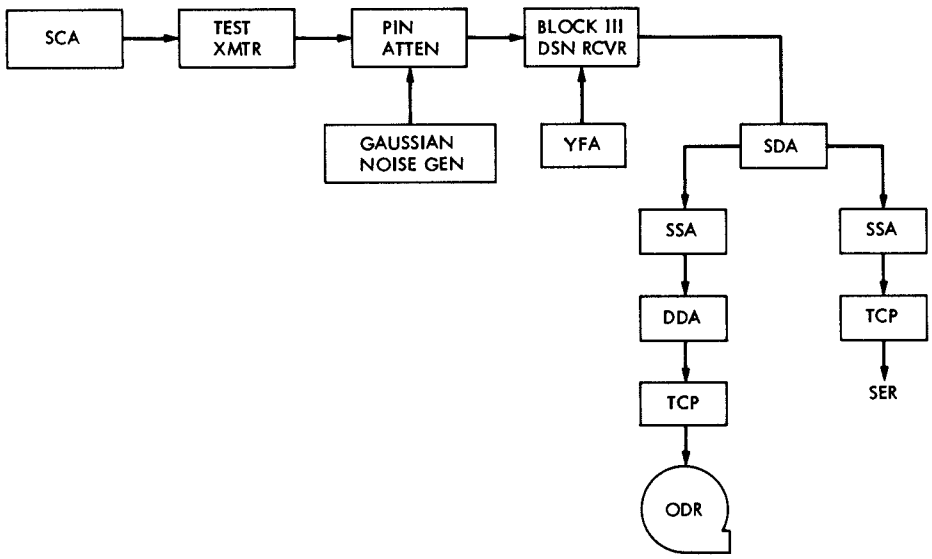

Fig. 1. Test configuration for PV78 sequential decoding tests in CTA 21

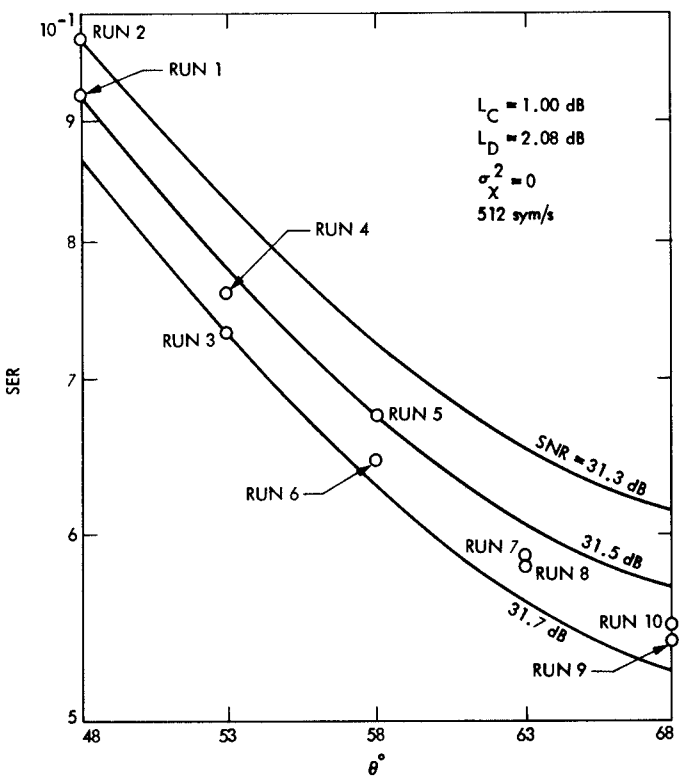

Fig. 2. Theoretical relationship between symbol error rate (SER) and modulation index θ for given received signal-to-noise ratio (SNR). Curves are for uncoded binary data at 512 symbols/s with no fading ($\sigma_X^2 = 0$).

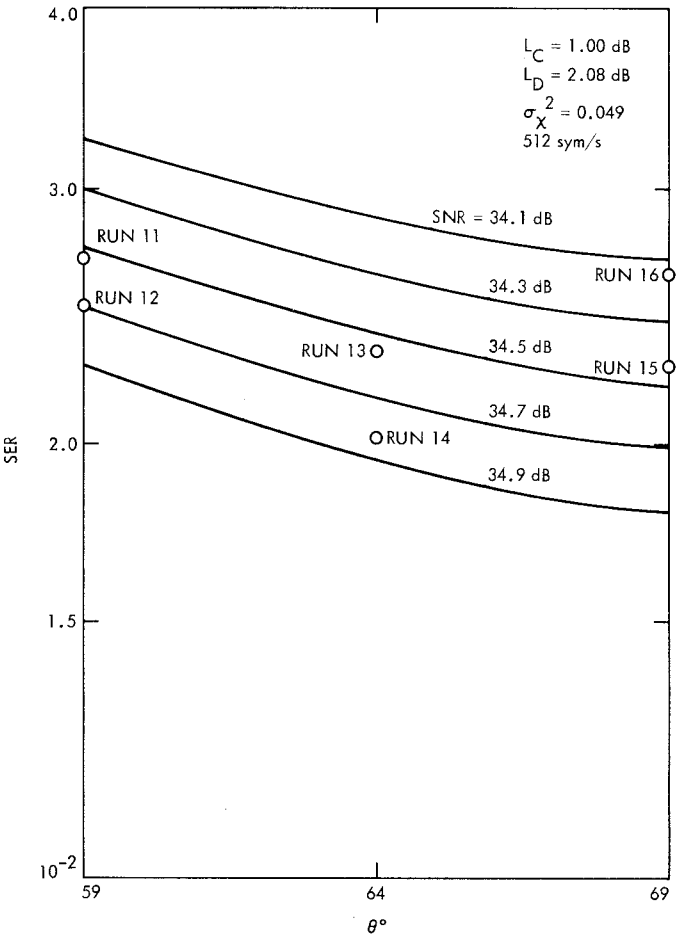

Fig. 3. Same as Fig. 2 , except for lognormal fading with $\sigma_X^2 = .049$

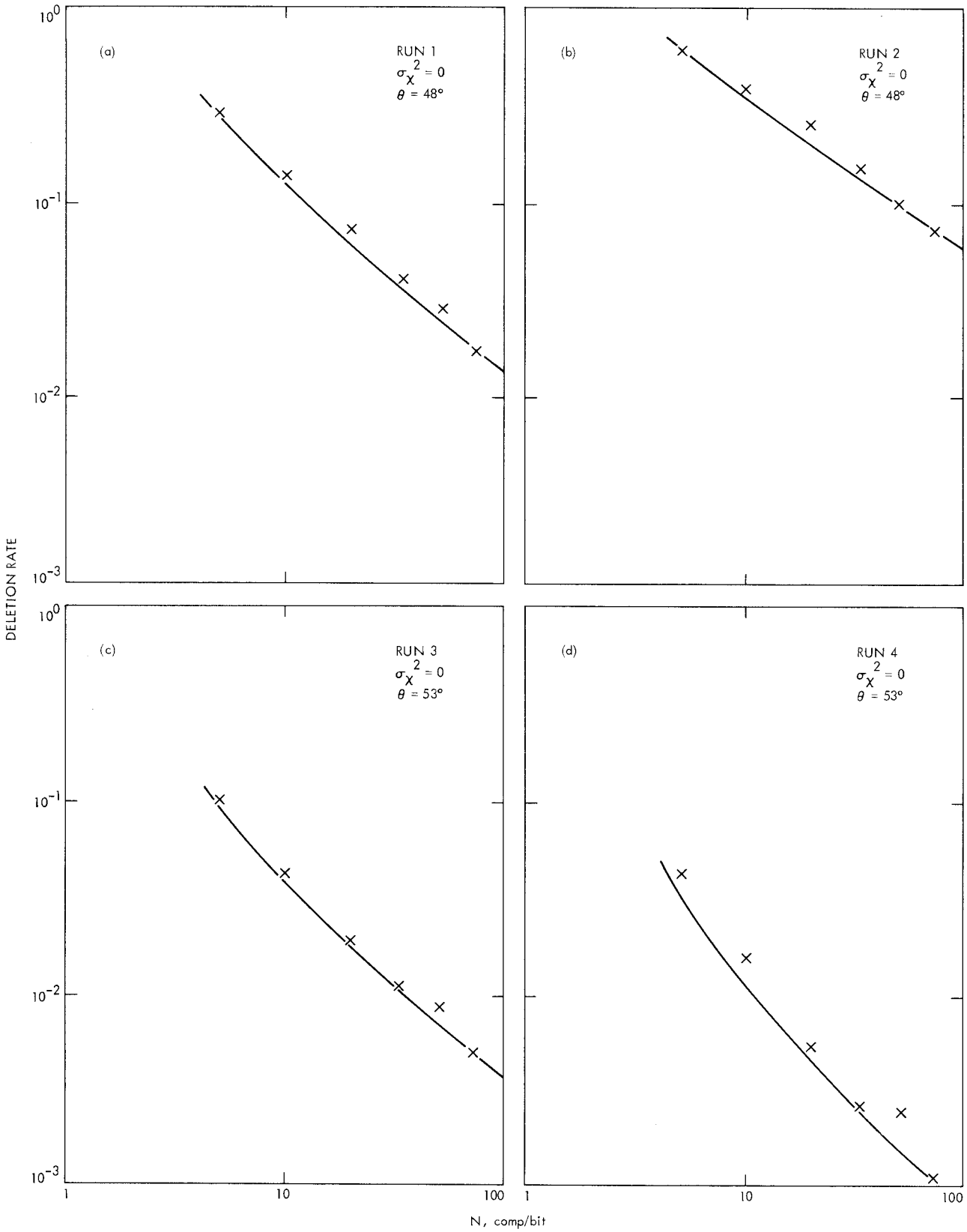

Fig. 4. Frame deletion rate test results

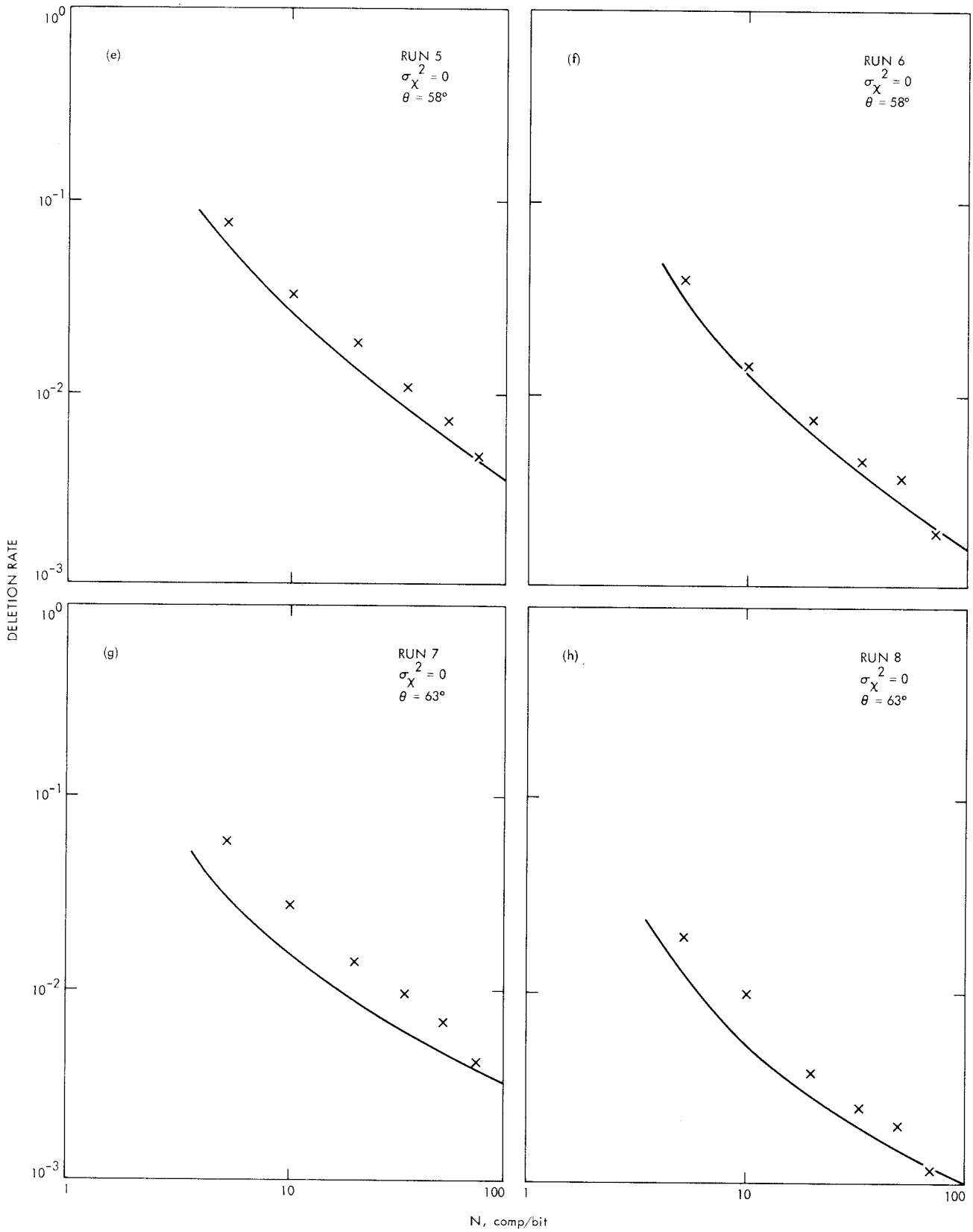
(e)
RUN 5
$\sigma_X^2 = 0$
$\theta = 58°$
(f)
RUN 6
$\sigma_X^2 = 0$
$\theta = 58°$
(g)
RUN 7
$\sigma_X^2 = 0$
$\theta = 63°$
(h)
RUN 8
$\sigma_X^2 = 0$
$\theta = 63°$
DELETION RATE
10^0
10^{-1}
10^{-2}
10^{-3}
1
10
100
N, comp/bit

Fig. 4 (contd)

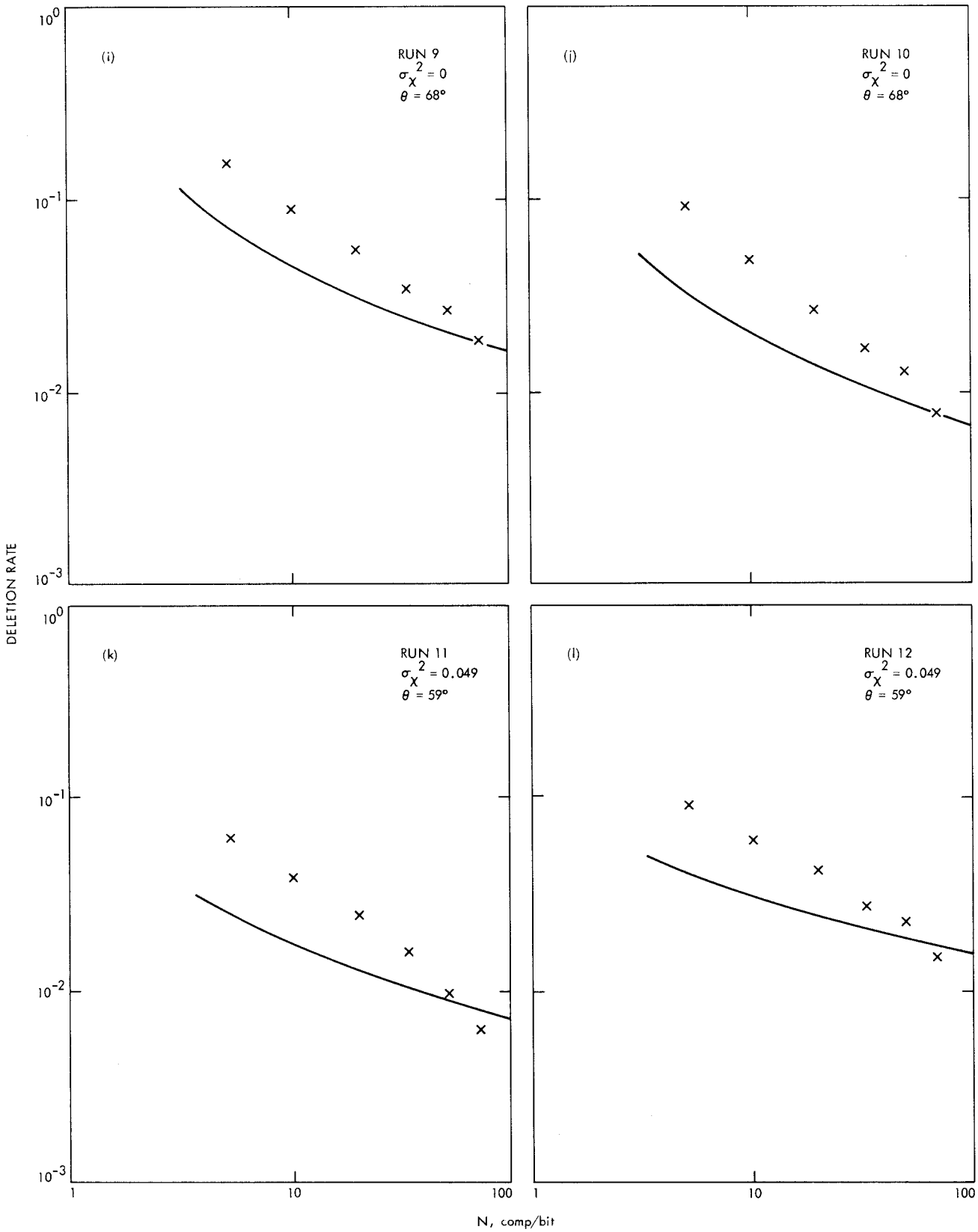
(i)
RUN 9
$\sigma_\chi^2 = 0$
$\theta = 68°$
(j)
RUN 10
$\sigma_\chi^2 = 0$
$\theta = 68°$
(k)
RUN 11
$\sigma_\chi^2 = 0.049$
$\theta = 59°$
(l)
RUN 12
$\sigma_\chi^2 = 0.049$
$\theta = 59°$
DELETION RATE
10^0
10^{-1}
10^{-2}
10^{-3}
1
10
100
N, comp/bit

Fig. 4 (contd)

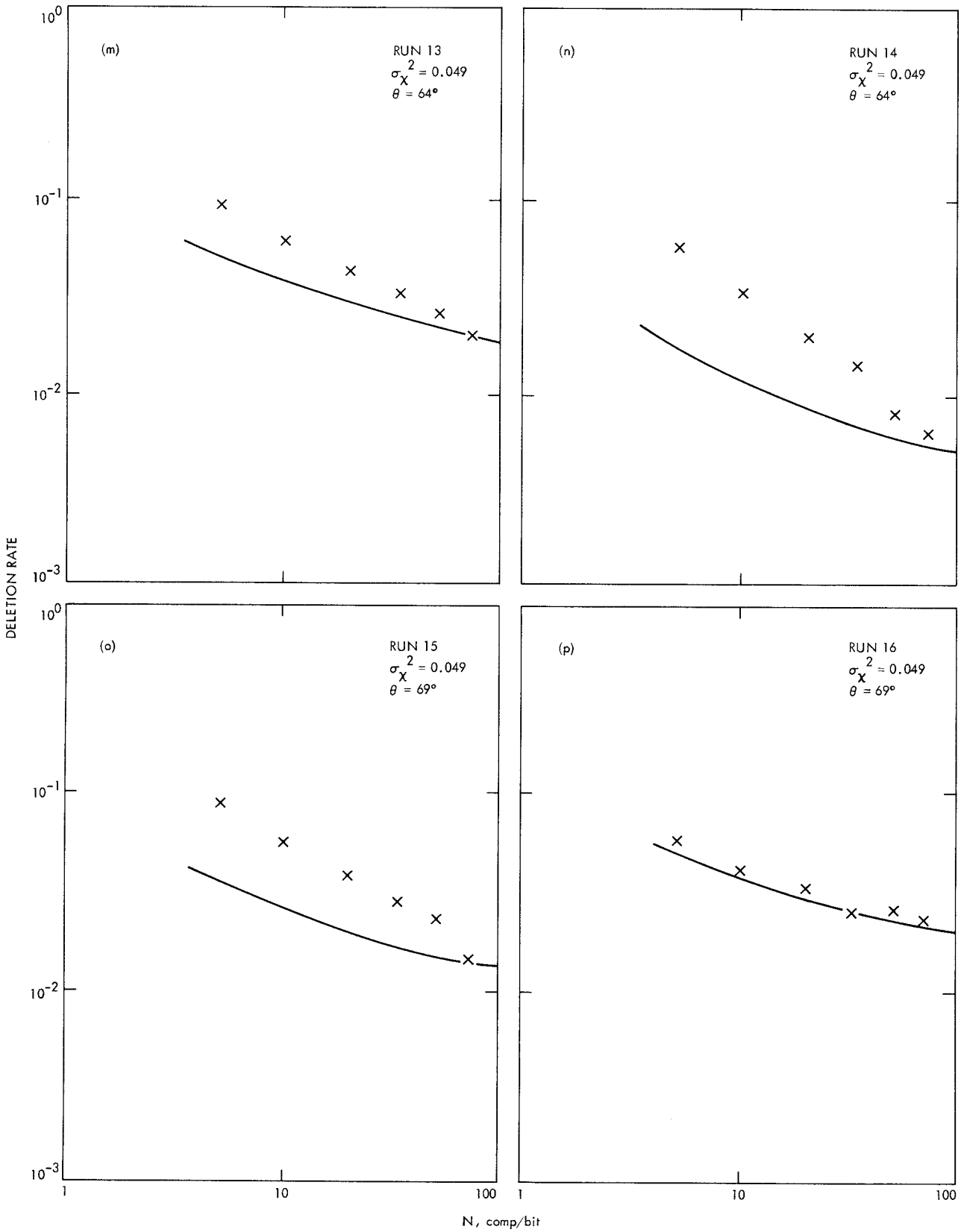
(m)
RUN 13
$\sigma_x^2 = 0.049$
$\theta = 64°$
(n)
RUN 14
$\sigma_x^2 = 0.049$
$\theta = 64°$
(o)
RUN 15
$\sigma_x^2 = 0.049$
$\theta = 69°$
(p)
RUN 16
$\sigma_x^2 = 0.049$
$\theta = 69°$
DELETION RATE
10^0
10^{-1}
10^{-2}
10^{-3}
1
10
100
N, comp/bit

Fig. 4 (contd)

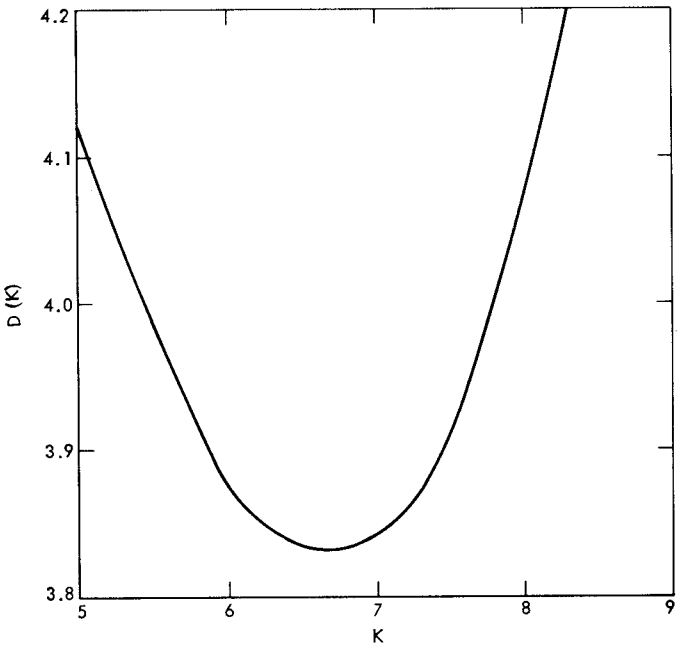

Fig. 5. Determination of $K = \lim_{N \to \infty} T_m / T_b$ for best agreement between empirical sequential decoding performance models and experimental data, based on distance parameter D

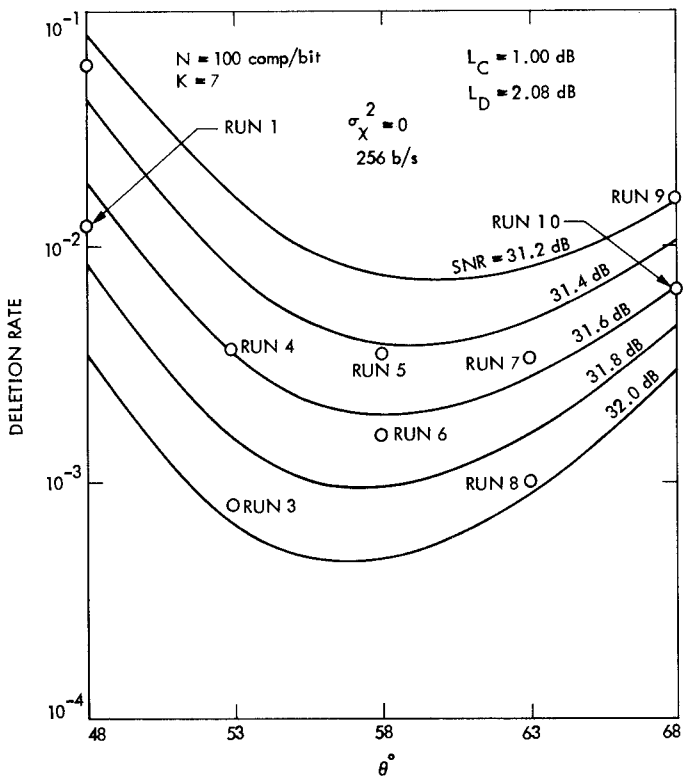

Fig. 6. Sequential decoding performance at 256 b/s with no fading ($\sigma_\chi^2 = 0$) based on empirical model with parameter $K = 7$.

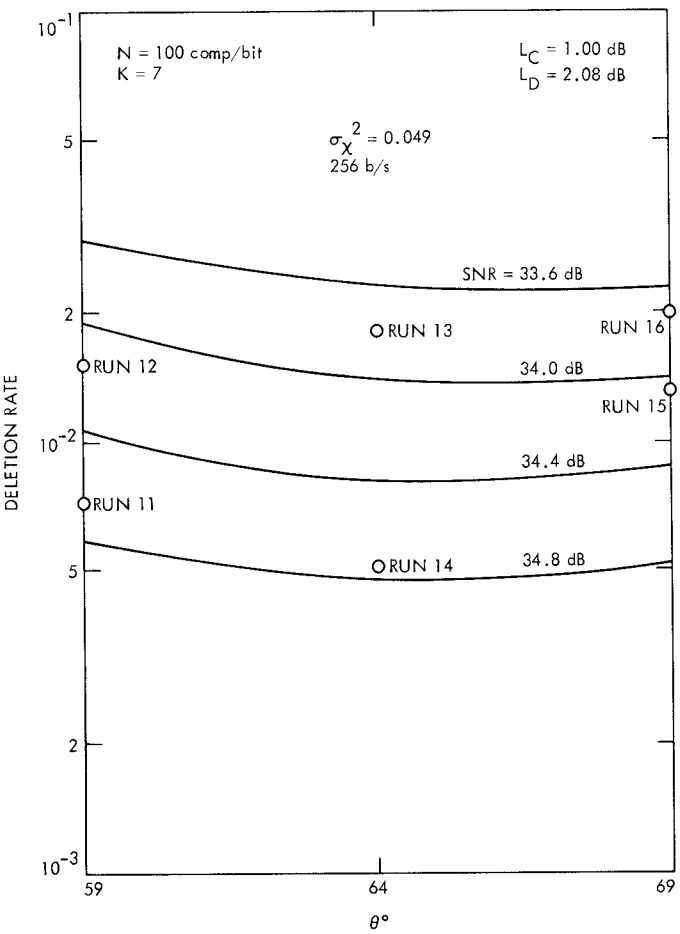

Fig. 7. Same as Fig. 6 , except for lognormal fading with $\sigma_\chi^2 = .049$.

Appendix

Lognormal Fading Simulation

Due to atmospheric fading, PV78 received telemetry will exhibit a time-varying lognormal envelope of the form $Ae^{\chi(t)}$ (Ref. 2, Eq. 2), where $\chi(t)$ is a Gaussian random process, with $\overline{\chi} = -\sigma_\chi^2$ based on conservation of energy arguments (i.e., $\overline{e^{2\chi}} = 1$). In db, the received amplitude has the form

$$a(t) = 20 \log_{10} A + (20 \log_{10} e)\, \chi(t) \text{ dB} \qquad \text{(A-1)}$$

In the absence of fading, $\chi(t)$ would be zero, and $a(t)$ would simply be $20 \log_{10} A$. With lognormal fading,

$$\overline{a} = 20 \log_{10} A - (20 \log_{10} e)\, \sigma_\chi^2$$

$$\sigma_a = (20 \log_{10} e)\, \sigma_\chi \qquad \text{(A-2)}$$

The PIN attenuator inserted in the transmission path in the test configuration of Fig. 1 has an input/output characteristic of the type illustrated in Fig. A-1. The attenuator receives a d.c. input bias voltage b_0, selected in a relatively linear region of the characteristic. The Gaussian noise generator injects a zero-mean signal $n(t)$ about the d.c. bias point, at an RMS level σ_n. Denoting the slope of the attenuator characteristic at the d.c. operating point by m, its gain is given by

$$a(t) \cong a_0 + m\, n(t) \qquad \text{(A-3)}$$

provided σ_n is small enough to keep the attenuator in the linear region about a_0.

To simulate the non-fading channel, the noise generator is turned off, and $a(t) = a_0 = 20 \log_{10} A$. With the injection of $n(t)$,

$$\overline{a} = a_0;\ \sigma_a \cong m\, \sigma_n \qquad \text{(A-4)}$$

To simulate the fading channel, a comparison of Eqs. A-2 and A-4 shows that the RMS noise level should be set at

$$\sigma_n = \left(\frac{20 \log_{10} e}{m}\right) \sigma_x \qquad \text{(A-5)}$$

and the received signal strength should be reduced by $(20 \log_{10} e)\, \sigma_x^2$ dB.

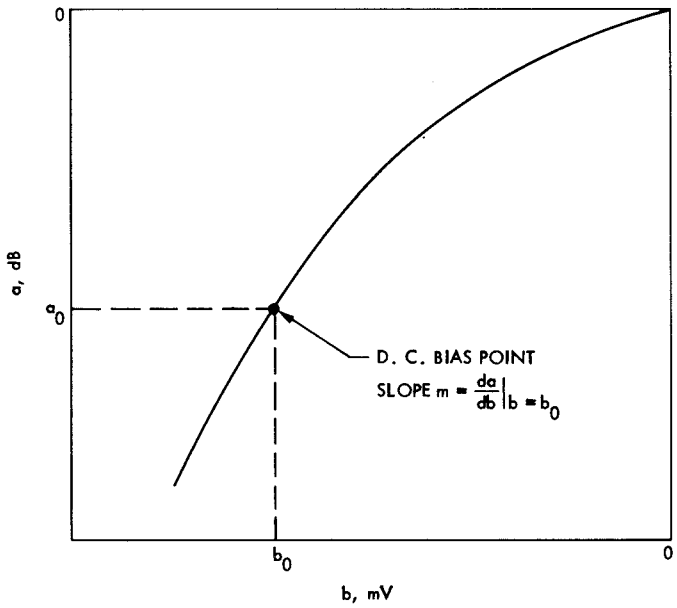

Fig. A-1. Form of PIN attenuator input/output characteristic